

Peter Albrecht¹

e-mail: albrecht@pi.tu-berlin.de

Stefanie Bade

e-mail: stefanie.bade@pi.tu-berlin.de

Arnaud Lacarelle

e-mail: arnaud.lacarelle@pi.tu-berlin.de

Christian Oliver Paschereit

Professor

e-mail: oliver.paschereit@tu-berlin.de

Hermann-Foettinger Institute (ISTA),
Technical University of Berlin,
D-10623 Berlin, Germany

Ephraim Gutmark

Distinguished Professor

Department of Aerospace Engineering and
Engineering Mechanics,
University of Cincinnati,
Cincinnati, OH 45221-0070
e-mail: ephraim.gutmark@uc.edu

Instability Control by Premixed Pilot Flames

Premixed flames of swirl-stabilized combustors (displaced half-cone) are susceptible to thermo-acoustic instabilities, which should be avoided under all operating conditions in order to guarantee a long service life for both stationary and aircraft gas turbines. The source of this unstable flame behavior can be found in a transition of the premix flame structure between two stationary conditions that can be easily excited by fuel fluctuations, coherent structures within the flow, and other mechanisms. Pilot flames can alleviate this issue either by improving the dynamic stability directly or by sustaining the main combustion process at operating points where instabilities are unlikely. In the present study, the impact of two different premixed pilot injections on the combustion stability is investigated. One of the pilot injector (pilot flame injector) was located upstream of the recirculation zone at the apex of the burner. The second one was a pilot ring placed at the burner outlet on the dump plane. A noticeable feature of the pilot injector was that an ignition device allowed for creating pilot premixed flames. The present investigation showed that these premixed pilot flames were able to suppress instabilities over a wider fuel/air ratio range than the conventional premixed pilot injection alone. Furthermore, it was possible to prevent instabilities and maintain the flame burning near the lean blow-out when a percentage of the fuel was premixed with air and injected through the pilot ring. NO_x emissions were significantly reduced. [DOI: 10.1115/1.3019293]

1 Introduction

The prevention and suppression of unstable combustion conditions in contemporary combustion chambers have to be guaranteed in all cases as otherwise the service life of the gas turbine can be dramatically reduced by pressure pulsations. Two main mechanisms are responsible for the development of instabilities: forced instabilities such as fuel or air mass flow fluctuations and self-driven instabilities such as thermo-acoustic instabilities. Besides geometrical solutions for improving the dynamic stability, many investigations have been conducted to force stable conditions by secondary pulsed fuel injection (see, e.g., Refs. [1–3]). In most cases, the fuel is modulated by injection valves with mechanical parts that may erode over time. Therefore, actuators that can support the active control methods are desired, especially for aircraft gas turbines with high safety standards. The control of the fuel split in the burner by piloted local fuel injections may be seen as a control method that fulfills these criteria.

Pilot flames may be used in two different ways to prevent instabilities:

1. The pilot flame is used directly to suppress the combustion instabilities, possibly changing the operating point of the burner.
2. The pilot flame is used to move the operating point of the burner to a more stable domain, which could be near the lean blowout (LBO) limit of the burner as reported by some authors.

As stated by different authors, the dynamic stability of the main combustion can be improved by the use of pilot flames. For example, Nair and Lieuwen [4] showed on a simplified burner geometry that pilot flame cannot only reduce the amplitude of pressure oscillations but also stabilize the overall combustion zone for

equivalence ratio below the unpiloted limit. Even if not performed on a swirled configuration, these results may be applicable to more complex flows. An example of stabilization of swirling combustor may be taken from Paschereit et al. [5]. The authors could stabilize the flow over a wide operating range by adjusting the position and the fuel mass flow of the pilot injection. They also pointed out a possible disadvantage of the use of pilot flame regarding NO_x emissions, which increase as the pilot fuel mass flow increases. This increase is mainly due to a decrease in the mixing quality, which leads to locally diffusion-like flames. These flames generate hot spots favorable to thermal NO emissions. A further step to reduce NO_x was done by Kendrick et al. [6]. He used a pilot premixed flame where fuel and air were mixed well before the injection into the combustion chamber. They could stabilize the combustion process but the control authority was strongly dependent on the pilot equivalence ratio Φ_{pilot} .

One possible explanation for the improved dynamic stability by pilot flames can be derived from basic investigations by Bradley et al. [7]. They have shown in their work that instabilities become likely if the side recirculation zone (see Fig. 2) loses its stabilization effect on the premixed flame. Thus, the flame front oscillation might be more easily excited by the already existing pressure fluctuations under these conditions, i.e., especially at operating points where the transition of the flame structure takes place [8]. For this reason, the Rayleigh criterion (Eq. (1), Sec. 4.1) could be satisfied faster as less excitation energy is necessary to exceed the dissipation losses. He also noticed that the heat release rate within the shear layer increases at stable conditions and decreases at unstable conditions. Thus stabilization of the flame may be linked to a localized injection of fuel in the shear layer.

In some configurations (e.g., Refs. [8–10]), the amplitude of pressure oscillations in swirl-stabilized combustors decreases significantly when operated at leaner mixtures (low Φ_{main}). Seo [10] explained this behavior by low heat release fluctuations near lean blowout so that flame instabilities are less likely. The mechanisms, however, are still unclear.

Thus according to previous works, a study of the effectiveness

¹Corresponding author.

Manuscript received February 25, 2008; final manuscript received August 25, 2008; published online January 12, 2010. Review conducted by Dilip R. Ballal. Paper presented at the ASME Turbo Expo 2008: Land, Sea and Air (GT2008), June 9–13, 2008, Berlin, Germany.

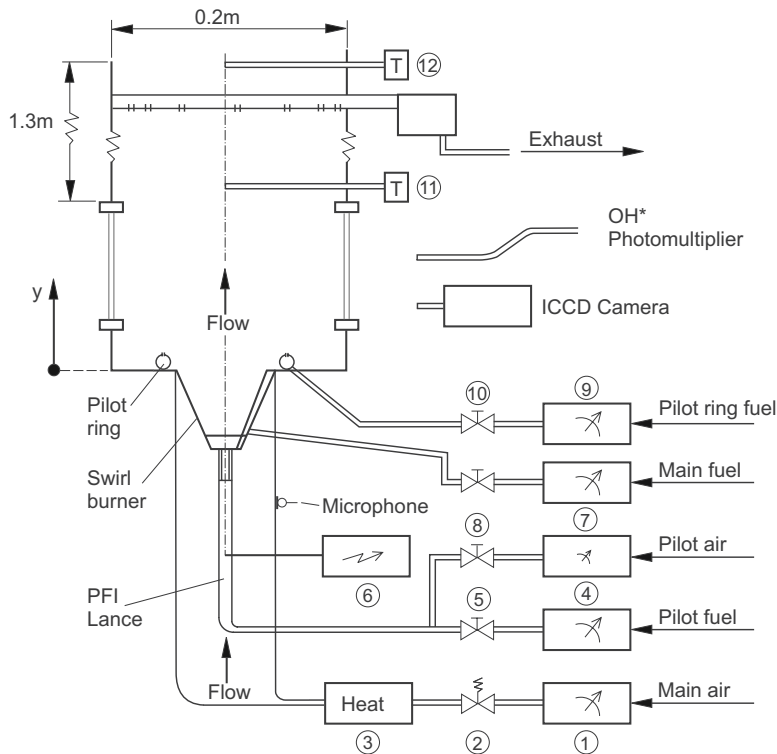


Fig. 1 Test rig facility and the swirl-stabilized combustor: (1) laminar flow element, (2) pneumatic slide valve, (3) heat exchanger, (4+7) mass meter, (5+8+10) needle valve, (6) high voltage ignition system, (9) rotameter, (11) thermocouple for bottom exhaust temperature, (12) thermocouple for exit exhaust temperature

of a pilot flame will have to take into account the two dominant parameters that seem to influence the pulsation behavior of the main combustion:

1. the heat release rate \dot{Q} within the shear layer between both recirculation zones
2. the equivalence ratio Φ_{main} of the main combustion

In the present study, the effectiveness of two pilot flame injections on the stability of a swirl premixed burner is investigated. In the first part, the test rig is presented as well as the two injection configurations: a premixed pilot injection that is able to be ignited is mounted at the apex of the burner, just upstream of the stagnation point of the center recirculation zone, and a pilot ring (PR) placed at the burner outlet on the dump plane. The description of the different injection configurations is shown in Sec. 3. The basic behavior of the combustor is described in Sec. 4. The results of the different injection configurations are shown in Sec. 5. They clearly showed that an increase in flame stabilization is achievable for some of the configurations tested.

2 Combustion Facility

The behavior of the emissions and the pressure oscillations near lean blowout were investigated with a swirl-stabilized combustor that was vertically mounted in the atmospheric test rig facility, as shown in Fig. 1. The swirl burner featured two axial slots formed by two shifted half-cones of 82 mm diameter through which air was forced in a circumferential direction (see Ref. [11] for more details). Natural gas was used as fuel and injected along the slots through 62 equally distributed 0.7 mm diameter boreholes. Thereby a homogeneous distribution of the mixture could be achieved at the outlet of the swirl burner where the side and central recirculation zones were generated by the strong swirling flow (Fig. 2). The premixed flame was able to anchor at that position so

that no additional flame holder was needed. Furthermore, the swirl burner has an opening at its apex where the pilot flame injector (PFI) lance was positioned for continuous fuel/air mixture injection. The PFI lance, discussed in Sec. 2.2 in detail, features an embedded sparkplug that is able to ignite the mixture periodically.

2.1 Atmospheric Test Rig Facility. For the investigation of emissions and pressure oscillations behavior near lean blowout, a quartz glass combustion chamber was used, 0.3 m in height and 0.2 m in diameter.

A 1.3 m tube extension (resonance tube) with the same diameter as the combustion chamber was mounted above the quartz glass. To record the amplitude of pressure oscillations, a water-cooled condenser microphone was mounted 0.4 m upstream of the burner outlet plane. A sample rate of 4096 Hz was set, and a low-pass filter at half of the sample rate was used. The pilot fuel and the main fuel were measured using a Coriolis mass meter, while the air mass flow was measured by a laminar flow element. All mass flows were set by metering valves that allowed a constant mass flow within a tolerance of less than 5%. Several k-type thermocouples with a 1.5 mm diameter were used to monitor the temperature of the preheated air upstream, the bottom exhaust temperature at 0.7 m, and the exit exhaust temperature at 1.48 m downstream of the dump plane. The water-cooled emissions probe was located 0.75 m downstream from the burner exit and had distributed openings to average the emissions across the exhaust duct. A heated flexible tube with a length of 12 m was used to lead the emissions into an analysis system, where NO and NO₂ were measured wet and CO, CO₂, and O₂ were measured dry. All emissions results presented in this study are based on 15 vol % O₂ and dry conditions. A constant exhaust mass flow of 55 l/h was set.

An OH*-photomultiplier (Hamamatsu, Arzbergerstr. 10, D-82211 Herrsching am Ammersee, Germany, H5784-03) and an Intensified Charged Coupled Device (ICCD) camera (Imager In-

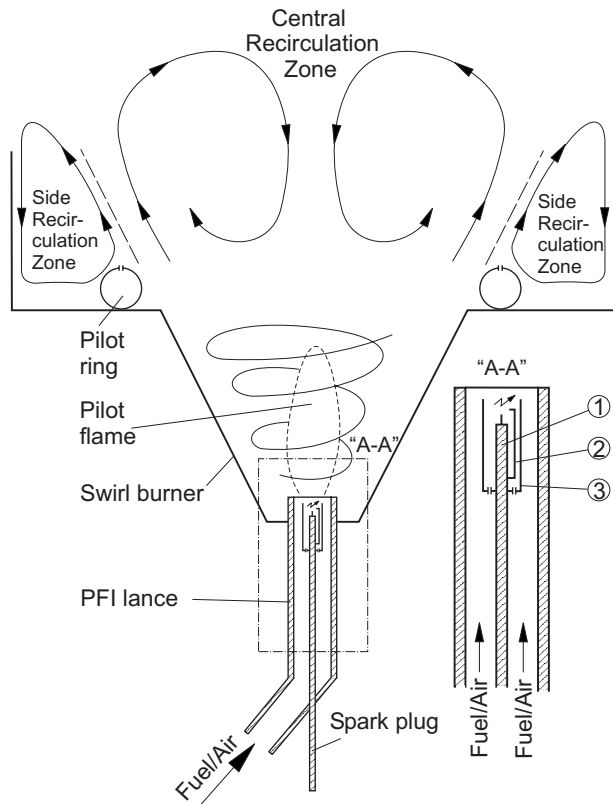


Fig. 2 PFI installation at the cone vertex and Pilot Ring at the combustor's dump plane. Insert shows the prototype of the PFI: (1) sparkplug, (2) ground electrode, and (3) ceramic tube.

tense, La Vision, Anna-Vandenhoeck-Ring 19, D-37081 Goettingen, Germany) equipped with a bandpass filter centered at 312 ± 2 nm were used to measure the fluctuations of the heat release rate and to visualize the flame front at unstable conditions. The ICCD camera was located 1.4 m in front of the combustion test rig center axis (see Fig. 6), and a fiber optic cable connected to the photomultiplier was mounted very close to the quartz glass combustion chamber (0.1 m) and 0.2 m above the combustor dump.

2.2 Pilot Flame Injector. The PFI was positioned in the center of the swirl burner apex and consisted mainly of a tube with an open end and a centered sparkplug (see Figs. 1 and 2). Fuel and air were mixed approximately 1.5 m before being led into the 1.2 m long PFI tube, so that a homogeneous mixture could be achieved at the PFI outlet. The premixed pilot flame could only be stabilized with the presence of a spark as the mixture velocity was set higher than the flame velocity so that the pilot flame could be directly controlled by the sparkplug.

Preliminary tests with the PFI have shown its capability to produce periodically generated premixed pilot flames under atmospheric conditions (see also Ref. [12]). The spark frequency at nonpreheated and preheated main air mass flows was 110 Hz. At this frequency, periodical ignition of the pilot fuel/air mixture could be accomplished within the investigated operating range.

2.3 Pilot Ring. The 110 mm diameter pilot ring was made out of a stainless steel tube, which was mounted on the burner dump plane (see Fig. 2). The 6 mm diameter tube was equipped with nine equidistantly distributed 1 mm diameter fuel injectors. The fuel injection was directed axially into the shear layer of the two recirculation zones.

Table 1 Investigated cases *without* pilot ring injection. All cases with PFI injection were conducted with 7.5 kg/h PFI air mass flow rate at $\Phi_{PFI}=1.1$.

Cases	Preheat temperature (K)	Outlet diameter (mm)	PFI injection (-)
Baseline-550 K	550	200	No
PFI-550 K	550	200	Yes
PFI-550 K-65 mm	550	65	Yes
PFI-300 K	300	200	Yes

3 Test Setup

The tests were conducted at a constant main air mass flow rate of 200 kg/h with 300 K (nonpreheated) and 550 K preheated main air temperatures, while the equivalence ratio Φ_{main} , the Φ_{PFI} , and Φ_{ring} were varied. Different combustor exit conditions were chosen to control the acoustic reflection coefficient r from fully open and reflecting down to $|r| < 0.3$. The test rig at a full reflecting coefficient had an outlet diameter of 200 mm, while the low reflection configuration had an outlet of 65 mm.

3.1 Test Cases Without Pilot Ring Injection. The pilot air mass flow rate of 7.5 kg/h through the PFI was kept constant throughout the investigation without pilot ring injection, while $\Phi_{PFI}=1.1$ was maintained. The integrated sparkplug within the PFI was switched off for the basic investigation described in Sec. 4, so that the pilot flame would not ignite. Therefore, the flame front of the main combustion was always located above the burner exit when the sparkplug was switched off.

Four different test cases were chosen to investigate the basic lean premixed flame behavior at different Φ_{total} and are summarized in Table 1. The cases "PFI-300 K" and "PFI-550 K" were repeated with PFI flames to investigate the direct influence of the PFI flame on combustion instabilities (Sec. 5).

3.2 Test Cases With Pilot Ring Injection. Four different cases shown in Table 2 were investigated to understand the impact pilot ring injection on the dynamic stability. To differentiate the cases they are identified by numbers representing the PFI air and fuel mass flows in kg/h and PR air and fuel mass flows in kg/h. For example, "baseline" represents the baseline case without pilot ring injection. A small amount of air (PFI air) was always used to cool the sparkplug. To generate premixed pilot ring flames, a constant pilot ring mixture of 15 kg/h air and 0.96 kg/h fuel was injected through the pilot ring (case "premixed ring"). For diffusion flame generations, the same fuel mass flow rate was injected through the pilot ring (case "diffusion ring").

4 Basic Behavior of the Swirl-Stabilized Premixed Flame Without Pilot Flames

The stability map for the different cases defined in Sec. 3.1 is shown in Fig. 3. While thermo-acoustic instabilities occurred for the cases with the 200 mm diameter combustor outlets, the case

Table 2 Investigated cases *with* pilot ring injection. All test cases were conducted at a main air preheat temperature of 550 K.

Cases	PFI air (kg/h)	PFI fuel (kg/h)	PR air (kg/h)	PR fuel (kg/h)
Baseline	1	0	0	0
Premixed ring	1	0	15	0.96
Diffusion ring	1	0	0	0.96
Air ring	1	0	15	0

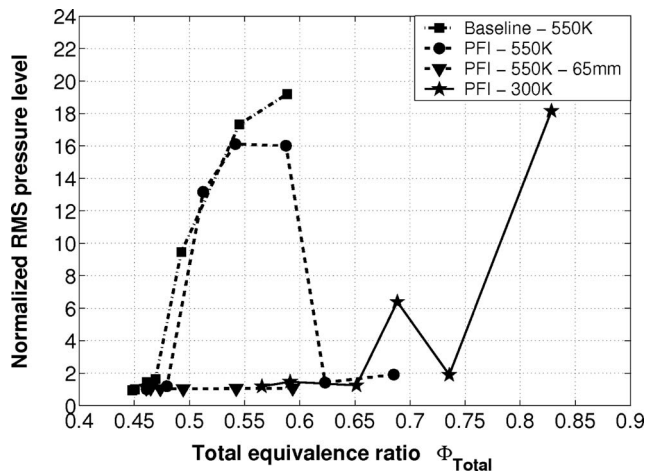


Fig. 3 Stability map of a swirl-stabilized combustion for different preheat air temperatures of 300 K and 550 K and combustion outlet diameters of 65 mm and 200 mm. The ignition device was in all cases off, so that no PFI flame was generated.

conducted with the 65 mm orifice remained stable within the whole investigated operating range and became unstable only close to the LBO, independent of the preheat temperature. At those points low frequency pressure oscillations at 3–7 Hz could be detected. The cause is possibly an incomplete combustion where fuel/air mixture pockets are ignited close to the hot inner walls and hot exhaust gases. The amplitudes of the rms pressure level for the “baseline-550 K” case were very low near lean blow-out at $\Phi_{total} \leq 0.47$ but increased significantly with increasing Φ_{total} .

The PFI-550 K case showed high level thermo-acoustic instabilities at $0.47 \leq \Phi_{total} \leq 0.6$. Out of this region, i.e., extremely close to the lean blowout limit and at condition $\Phi_{total} > 0.6$, the combustion was stable. The PFI-300 K case showed unstable conditions with a high rms pressure level at $\Phi_{total} > 0.67$.

4.1 Rayleigh Index. The instabilities found for the cases PFI-550 K and PFI-300 K were more closely investigated to better quantify the intensity of the instabilities. The OH-chemiluminescence (OH^*) and the pressure fluctuations p' of the oscillating premixed flame were simultaneously recorded, as shown in Fig. 4 for the PFI-550 K case at $\Phi_{total}=0.55$. The phase

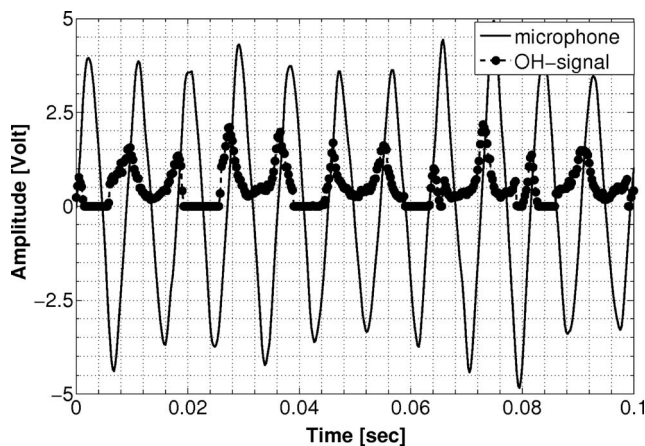


Fig. 4 OH-chemiluminescence and pressure signals for the case PFI-550 K at $\Phi_{total}=0.55$

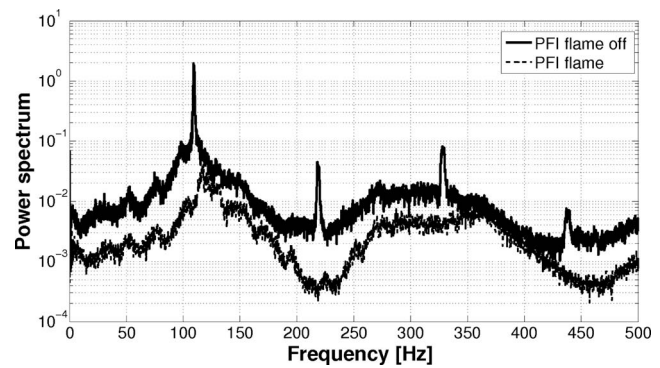


Fig. 5 Power spectrum for the case PFI-550 K with and without PFI flame at $\Phi_{total}=0.55$

shift of less than 90 deg between these two signals indicates clearly unstable conditions. Also the Rayleigh index R , calculated by the formula

$$R = \int_0^{\text{time}} p'(t) \cdot (OH^*)(t) dt > \text{dissipation losses} \quad (1)$$

was fulfilled.

4.2 Power Spectrum and Phase-Averaged OH-Chemiluminescence. The power spectrum for the case PFI-550 K shows a distinct fundamental at 110 Hz with an amplitude nearly three orders of magnitude higher than the background noise (Fig. 5). To visualize the oscillating character of the unstable lean premixed flame for the PFI-300 K case at $\Phi_{total}=0.66$, phase-averaged OH^* images were recorded in 45 deg steps, while the images for each phase shift angle were calculated from 40 single images (Fig. 6). At 45 deg the highest OH^* -chemiluminescence can be detected within the shear layer between the side and central recirculation zones.

4.3 Hysteresis Effect. A hysteresis effect described in several papers (e.g., Refs. [13,10]) was not clearly detected when investigating the pulsation behavior in both direction, from a rich to a lean mixture and vice versa (Fig. 7).

4.4 Heat Release Visualization for Different Operating Points. OH^* -chemiluminescence was also measured at different operating conditions shown in Fig. 7. Assuming that the heat release is qualitatively related to the OH^* -chemiluminescence, the highest heat release rate at $\Phi_{total} \geq 0.6$ could be detected within the shear layer between the side and central recirculation zones (Fig. 7). The highest heat release rate at $\Phi_{total} \leq 0.5$ close to the lean blowout was approximately one combustor diameter downstream of the swirl burner exit. With increasing Φ_{total} , the maximum heat release zone moved further upstream. The right side of the combustor flame seemed to be more intense in all cases, but this could be attributed to the arrangement of the camera position and the swirl-stabilized burner. In this study, the cross section of the combustor outlet air slots were located at a 45 deg angle to the camera, as can be seen in Fig. 6.

5 Strategies for Suppressing Combustion Instabilities With Pilot Flames

Two different ways to suppress instabilities that were described in Sec. 4 are presented here. In Sec. 5.1, it will be shown that premixed pilot flames generated by the PFI are able to suppress and directly control the instabilities. However, the improved dynamic stability could only be proven for a continuous PFI air mass flow rate of 7.5 kg/h at $\Phi_{PFI}=1.1$. Test results in Sec. 5.2 show that the ring injection of both fuel and air affects significantly the

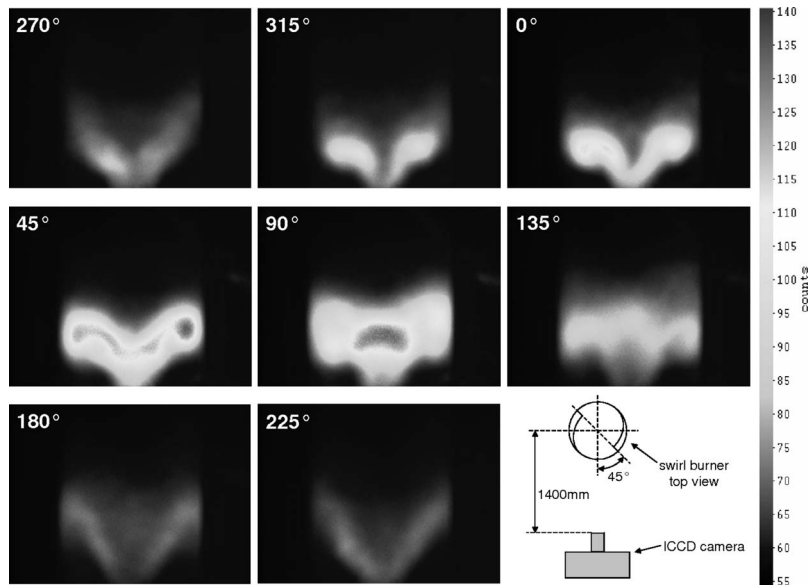


Fig. 6 Phase-averaged OH-chemiluminescence images at different phase shift angles at 200 kg/h main air mass flow rate and 300 K nonpreheated air for $\Phi_{\text{total}}=0.66$. The instability occurred at 82 Hz.

pressure oscillation of the main combustion and is caused mainly by a higher jet momentum through the pilot ring.

5.1 Active Control of Instabilities. Preliminary tests were performed to investigate the effectiveness of the PFI lance. In the following, we will only show operating conditions that were effective (see Figs. 8–11). All rms pressure levels were normalized by the background noise of the baseline case baseline-550 K at $\Phi_{\text{total}}=0.45$. The test conditions of the results presented in this section are shown in Sec. 3.1.

5.1.1 Response Behavior for PFI Flame On/Off Conditions. Two highly unstable conditions were chosen for the investigation at $\Phi_{\text{total}}=0.55$ and at 0.58 for 550 K preheated air and another highly unstable condition at $\Phi_{\text{total}}=0.66$ for nonpreheated air. The 550 K case is shown in Fig. 8. During the first 12 s, the PFI spark was off, and only a small amount of premixed fuel was injected

(without PFI flame). This was not enough to suppress the instabilities. Then, a periodic PFI flame was generated by the PFI spark, and the instability was completely suppressed. Instabilities at $\Phi_{\text{total}}=0.66$ for nonpreheated air could be suppressed when the sparkplug was activated, as can be seen in Fig. 9. Within the first 12 s, a PFI flame was generated by the activated sparkplug, and the rms pressure level could be held to a very low level. Even though the sparkplug was switched off after 12 s, the combustion remained in a stable mode for approximately 6 s before becoming unstable. After 56 s, the sparkplug was activated again, and the instability was instantly suppressed. The time delay of several seconds between the switching off of the spark and the initiation of instabilities could be related to the fact that the flame front was stabilized inside of the swirl burner even though the PFI flame was already off.

5.1.2 Overall Dynamic Stability With PFI Flames. The instabilities shown for the cases PFI-300 K and PFI-550 K could be completely suppressed by the presence of the premixed PFI flame (Figs. 10 and 11). The PFI changed the heat release distribution within the flame front, as can be seen in Fig. 10, and thus affected the dynamic stability. The results are consistent with the investigation of Paschereit et al. [14].

5.1.3 Emissions. The impact of the instabilities on the emission behavior can be seen in Fig. 12, where the NO_x emissions were recorded at different operating conditions and plotted versus the total equivalence ratio (Φ_{total}). The curve referred to as “PFI flame-off” was recorded when the PFI fuel/air mixture was not ignited and therefore corresponds to PFI-550 K, as described in Sec. 4. Furthermore, the cases with activated PFI flame are referred to as “PFI flame” in the following.

With PFI flame, NO_x emissions were reduced when compared with the unstable baseline case. This is in agreement with Paschereit and Gutmark [15], who showed that unstable premixed combustion may increase NO_x emissions. It is interesting to note that the NO_x emissions between the PFI flame and the PFI flame-off case are similar in stable regions ($\Phi_{\text{total}} > 0.6$, compare Fig. 10), while the emissions significantly differ within the unstable region ($0.5 < \Phi_{\text{total}} < 0.6$). Therefore, higher NO_x emissions are generated mainly by flame temperature peaks (induced by fuel/air ratio oscillations) during thermo-acoustic instabilities and not by the PFI flame itself.

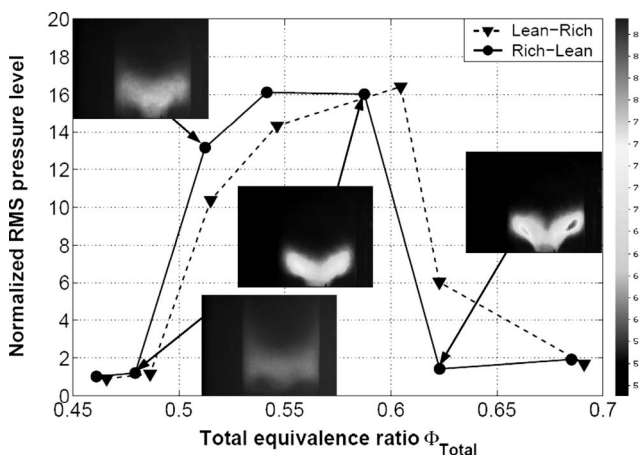


Fig. 7 OH-chemiluminescence images and rms pressure level at different operating points for the case PFI-550 K; the sparkplug was not activated. While for the curve “rich-lean,” the pressure fluctuations were investigated from a rich mixture to a lean mixture, and the rms pressure level was recorded for the curve “lean-rich” at the starting operating point Φ_{total} near lean blowout. A hysteresis effect was not clearly visible.

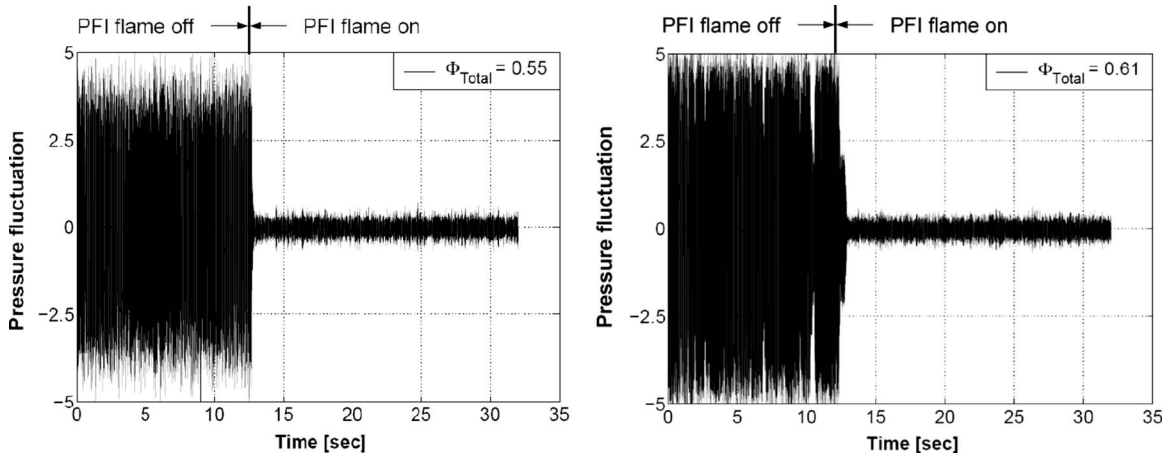


Fig. 8 Time signal of the pressure fluctuations for the case PFI-550 K at $\Phi_{total}=0.55$ and 0.61 with and without PFI flame. The frequency of the PFI flame was 110 Hz.

5.2 Passive Control of Instabilities. After having shown that the actively controlled pilot (PFI) could reduce significantly pressure pulsations and emissions, it was of further interest to investigate a premixed pilot located closer to the outer shear layer. A pilot ring was installed at the burner dump plane (Fig. 2), where

fuel or a fuel/air mixture could be injected directly into the shear layer. A detailed overview of the parameter setup used for this test and the definition of the cases can be found in Sec. 3.2.

5.2.1 Advantages of Premixed Pilot Ring Injection. In Fig. 13,

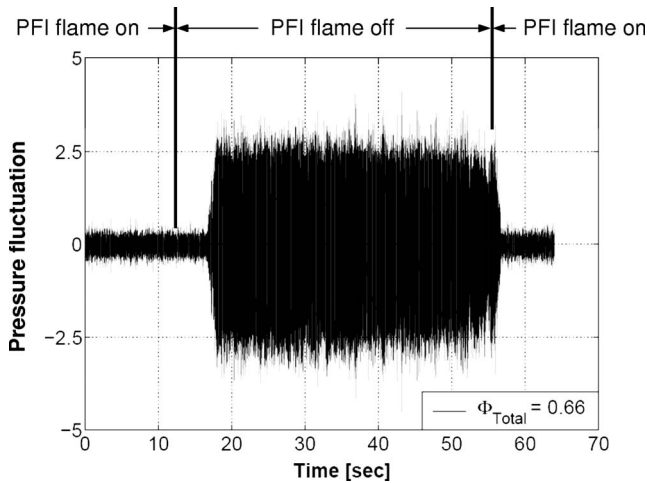


Fig. 9 Time signal of the pressure fluctuations for the case PFI-300 K with and without PFI flame at $\Phi_{total}=0.66$. The frequency of the PFI flame was 110 Hz.

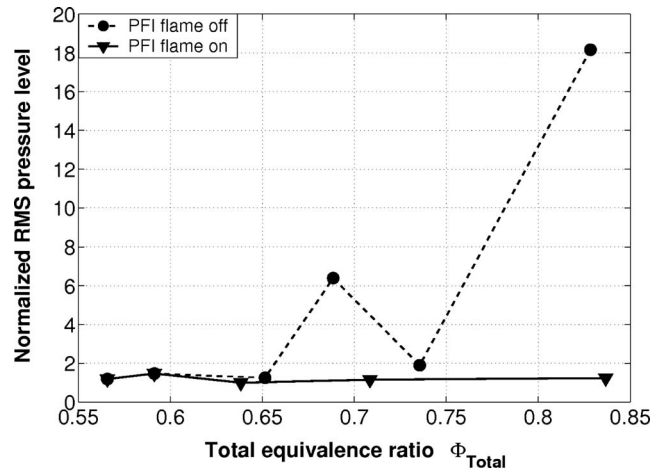


Fig. 11 rms pressure level for the case PFI-300 K with and without PFI flame. All rms values are normalized on the background noise of the baseline case at $\Phi_{total}=0.45$.

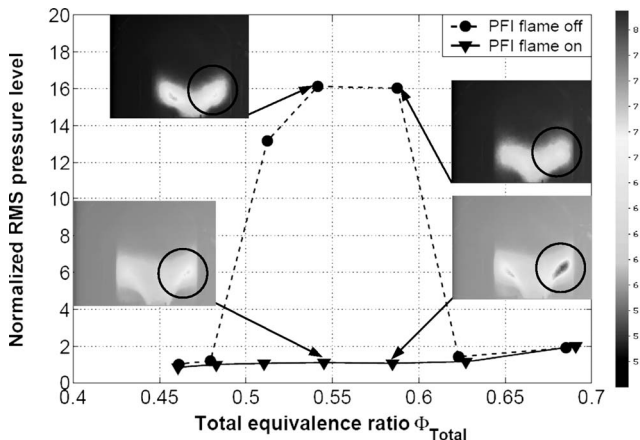


Fig. 10 Comparison of the OH-chemiluminescence between the side and central recirculation zones for the case PFI-550 K with and without PFI flame

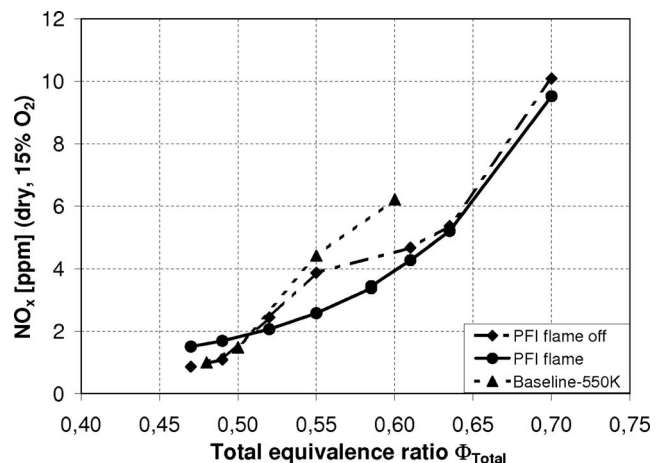


Fig. 12 NO_x emission for the case baseline-550 K and for the case PFI-550 K with and without PFI flame

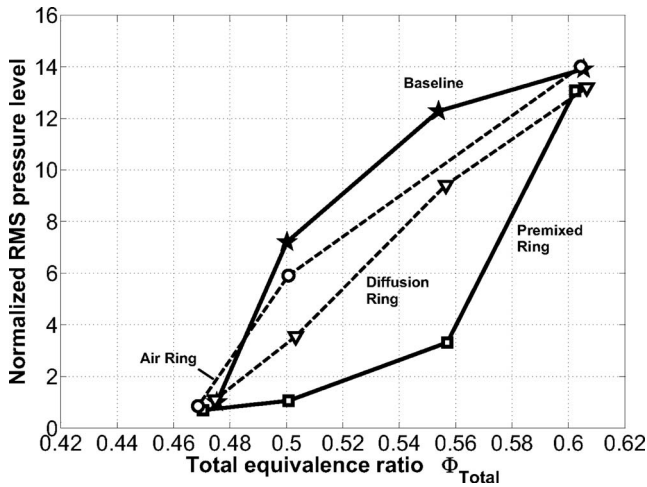


Fig. 13 Influence of the pilot ring flames (diffusion ring and premixed ring) on the normalized rms pressure level. All rms values were normalized on the background noise of the baseline case at $\Phi_{total}=0.45$.

the normalized rms pressure level versus Φ_{total} for different injected mass flows through the pilot ring is plotted. The data are normalized by the rms pressure level at $\Phi_{total}=0.47$ for the baseline case. Using the premixed pilot (premixed ring), the pressure pulsation increase at $\Phi_{total}>0.47$ of the baseline case could be delayed significantly with the premixed pilot to $\Phi_{total}>0.54$. Injecting the same amount of fuel through the pilot ring but without 15 kg/h air mass flow rate did not improve the dynamic stability to a higher Φ_{total} , as can be seen in the case of “diffusion pilot.” As expected, also the NO_x emissions were significantly higher when compared with the premixed ring case (Fig. 14). To visualize the impact of the different injection configurations on the flame shape, the averaged flame heat release was recorded with the ICCD camera, and the resulting pictures are plotted in Fig. 15. The pictures allow both to locate the axial flame position and to estimate the flame thickness, characterized by the spreading of the OH^* -chemiluminescence. All the cases, except the diffusion ring case, present stable flames, which are shifted downstream outside of the burner. A flame located further downstream involves an increase in the convective time delays of the fuel to the flame front. This induces a stabilization of the system as the time delays are not related anymore to characteristic times of the combustor unstable modes (the period of the instability for example). More-

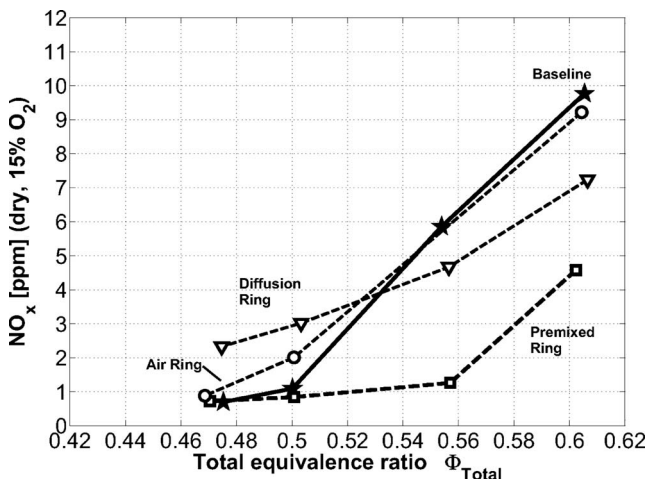


Fig. 14 NO_x emission for different pilot ring injection cases

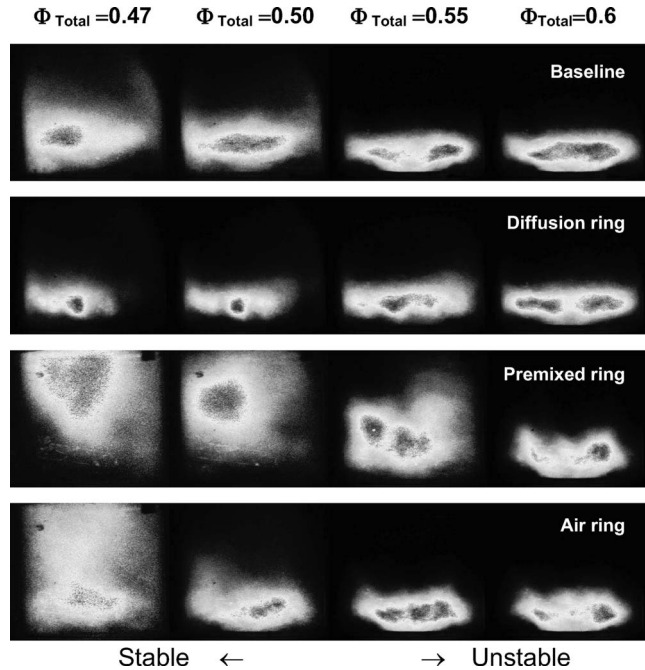


Fig. 15 Mean flame heat release of the four injection configurations depending on the total equivalence ratio Φ_{total}

over, stable flames show a stronger axial spread than unstable flames. A high spread is also linked with a high variance in the convective time delay distribution. Increasing its value is also a means to reduce the pulsation amplitude of a combustion system, as shown in Scarinci and Freeman [16]. The premixed ring case presents high values of both parameters over a much wider equivalence ratio range (up to $\Phi_{total}=0.55$) compared to the three other cases, correlating very well with the rms pulsations shown in Fig. 13. Thus, this case shows a positive impact on the two parameters relevant to the stability of the system.

5.2.2 Damping Mechanism. Two different phenomena help in understanding the beneficial effect of the premixed ring on the combustion stability: the leaner mixture of the main flame and the high momentum achieved through the ring injectors. First, injecting about 15% of the overall fuel mass flow through the ring yields a leaner mixture of the premixed main flame at constant total equivalence ratio. When the main flame approaches the lean blowout limit, a lift-off of the flame occurs, which stabilizes the system because of the higher convective time delays. Through the additional injection of fuel, the premixed ring allows us to perform combustion with a lifted flame over a wider equivalence ratio range Φ_{main} of the main flame. It helps thus to sustain the main flame combustion near and below its natural lean blowout limit. The second effect relates to the high momentum of the air injected through the ring. To further understand the mechanism, the impact of fuel ring injection and air ring injection on the main combustion are separately investigated. The results are presented in Fig. 16, where the rms pressure level deviation relative to the baseline case is plotted versus the main equivalence ratio Φ_{main} . While the air ring injection (“air ring”) damps significantly the rms pressure level of the main combustion when compared with the baseline, the fuel ring injection (diffusion ring) excites the pressure oscillations. The combined injection of fuel and air through the pilot ring (premixed ring) is able to keep the pressure oscillations below the baseline case but with lower damping effect when compared with the air ring. Obviously, the stabilization effect on the main combustion is mainly caused by the high momentum of the pilot ring jet and not by the heat release rate within the shear layer of both recirculation zones. The assumption is

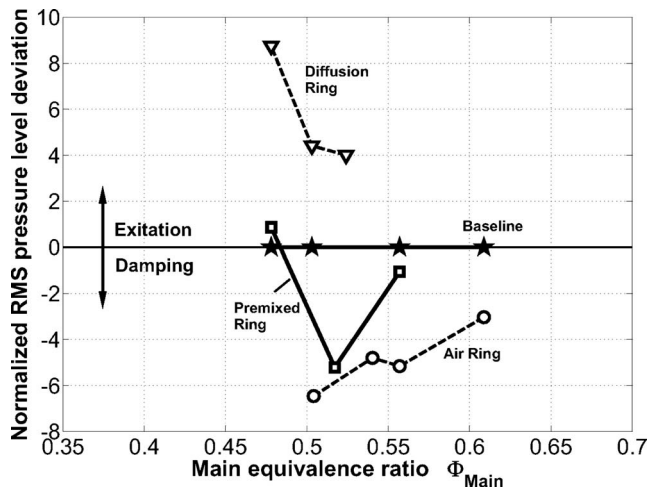


Fig. 16 Impact of different pilot ring injection cases on the main flame stabilization

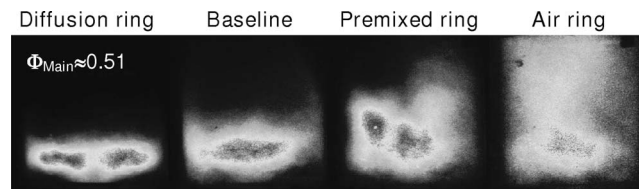


Fig. 17 Mean flame heat release of the four injection configurations

confirmed when looking at the OH^* images corresponding to $\phi_{\text{main}} \approx 0.51$ in Fig. 17. They confirm that the air ring injection has the most stabilizing effect at constant ϕ_{main} by increasing the spreading of the flame.

6 Conclusion

Active and passive control methods for instability suppression were successfully applied on a swirl-stabilized combustor. Stability maps of the combustor were recorded for different operating conditions. Unstable conditions were actively controlled by using a periodically ignited premixed flame. It reduced significantly pressure pulsations and NO_x emissions. Regarding the passive control method, a continuous premixed pilot ring injection located at the combustor dump plane show reduced pulsations and emissions. The damping effect is mainly achieved by the high jet momentum through the pilot ring. Moreover, the combined injection of fuel and air through the ring influences and sustains significantly the spreading and the lift-off of the main flame that appears to be another damping source for pressure oscillations.

Acknowledgment

We gratefully acknowledge the work of Willi Postel who has manufactured the PFI lance. Furthermore, we gratefully acknowl-

edge Tyler Jensen who helped us during preliminary tests of the PFI lance.

Nomenclature

- T_{CCW} = wall temperature of the combustion chamber
 OH^* = OH-chemiluminescence
 Φ_{total} = total equivalence ratio calculated from Φ_{main} and Φ_{PFI}
 Φ_{main} = main equivalence ratio of the main combustion
 Φ_{PFI} = equivalence ratio of the flame produced by the pilot flame injector
 Φ_{pilot} = equivalence ratio of the pilot flame
 p' = pressure fluctuation within the combustion chamber
 R = Rayleigh index

References

- [1] Candel, S. M., 1992, "Combustion Instabilities Coupled by Pressure Waves and Their Active Control," 24th Symposium (International) on Combustion, The Combustion Institute, pp. 1277–1296.
- [2] Hoffmann, S., Weber, G., Judith, H., Hermann, J., and Orthmann, A., 1998, "Application of Active Combustion Control to Siemens Heavy Duty Gas Turbines," Applied Vehicle Technology Panel Symposium, Lisbon, Portugal, Vol. 14.
- [3] Paschereit, C. O., Gutmark, E., and Weisenstein, W., 1999, "Control of Thermoacoustic Instabilities in a Premixed Combustor by Fuel Modulation," AIAA Paper No. 99-0711.
- [4] Nair, S., and Lieuwen, T., 2003, "Acoustic Detection of Imminent Blowout in Pilot and Swirl Stabilized Combustors," ASME Paper No. GT2003-38074.
- [5] Paschereit, C. O., Flohr, P., and Gutmark, E. J., 2006, "Combustion Control by Vortex Breakdown Stabilization," ASME J. Turbomach., **128**(4), pp. 679–688.
- [6] Kendrick, D. W., Anderson, T. J., Sowa, W. A., and Snyder, T., 1999, "Acoustic Sensitivities of Lean-Premixed Fuel Injectors in a Single Nozzle Rig," ASME J. Eng. Gas Turbines Power, **121**, pp. 429–436.
- [7] Bradley, D., Gaskell, P. H., Gu, X. Y., Lawes, M., and Scott, M. J., 1998, "Premixed Turbulent Flame Instability and NO Formation in a Lean-Burn Swirl Burner," J. Propul. Power, **21**(1), pp. 32–39.
- [8] Fritsche, D., 2005, "Origin and Control of Thermoacoustic Instabilities in Lean Gas Turbine Combustion," Ph.D. thesis, Swiss Federal Institute of Technology Zurich.
- [9] Lenz, M., 1998, "Experimentelle Optimierung des Stabilitätsverhalten von Gasturbinenbrenner," University Erlangen-Nuernberg, Chair of Technical Thermodynamics, Germany, Technical Report.
- [10] Seo, S., 1999, "Parametric Study of Lean Premixed Combustion Instability in a Pressurized Model Gas Turbine Combustor," Ph.D. thesis, Department of Mechanical and Nuclear Engineering, The Pennsylvania State University, University Park.
- [11] Keller, J., and Sattelmayer, T., 1991, "Double-Cone Burners for Gas Turbine Type 9 Retrofit Application," presented at the 19th International Congress on Combustion Engines (CIMAC), Florence.
- [12] Albrecht, P., Speck, S., Schimek, S., Bauermeister, F., Paschereit, C. O., and Gutmark, E., 2007, "Lean Blowout Control Using an Auxiliary Premixed Flame in a Swirl-Stabilized Combustor," AIAA Paper No. 2007-5632.
- [13] Lepers, J., Krebs, W., Prade, B., Flohr, P., Pollarolo, G., and Ferrante, A., 2005, "Investigation of Thermoacoustic Stability Limits of an Annular Gas Turbine Combustor Test-Rig With and Without Helmholtz Resonators," ASME Paper No. GT-2005-68246.
- [14] Paschereit, C., Schuermans, B., and Bueche, D., 2003, "Combustion Process Optimization Using Evolutionary Algorithm," ASME Paper No. 2003-GT-38393.
- [15] Paschereit, C. O., and Gutmark, E. J., 2008, "Combustion Instability and Emissions Control by Pulsating Fuel Injection," ASME J. Turbomach., **130**(1), pp. 12–19.
- [16] Scarinci, T., and Freeman, C., 2000, "The Propagation of a Fuel-Air Ratio Disturbance in a Simple Premixer and Its Influence on Pressure Wave Amplification," ASME Paper No. 2000-GT-0106.